

Synthesis of Fluorescent Rhodium(II) and Iridium(II) Complexes Promoted by 2,6-Bistetrazolate Pyridine Ligand

RAYEES AHMAD MALIK* and AMIT CHATTREE

Department of Chemistry, Faculty of Science, Sam Higginbottom University of Agriculture, Technology and Sciences, Allahabad-211007, India

*Corresponding author: E-mail: malikraqueeb123@gmail.com

Received: 16 August 2019;

Accepted: 22 November 2019;

Published online: 30 December 2019;

AJC-19741

Tridentate N-donor ligand 2,6-bistetrazolate pyridine (H_2pytz) has been prepared from 2,6-pyridinedicarbonitrile and used for coordination with transition metals $[M(pytz)_2](NH_4)_2$, ($M = Rh, Ir$). The structure of Rh and Ir complexes was determined by UV, FT-IR, 1H NMR, XRD and elemental analysis. Moreover, the absorption spectra of complexes were shifted towards the visible region (367.2 nm for Rh and 370.8 nm for Ir). The π -excessive, lone pair nitrogen donors and extended unsaturation of ligand triggers the visible fluorescence spectra upto 528.5 nm for rhodium complex and 557.5 nm for iridium complex. The antibacterial activity results revealed that *S. aureus* and *E. coli* showed maximum response followed by *K. pneumoniae* and *B. cereus*, respectively. The maximum zone of inhibition of complexes was observed at 6 mg/mL concentration viz. *S. aureus*, 15.0 ± 1.15 mm for rhodium complex and *E. coli*, 14.6 ± 1.15 mm for iridium complex. Therefore, 2,6-bistetrazolate pyridine (H_2pytz) ligand tune the photo-physical properties of the complexes as well as their applications in the biological fields.

Keywords: Rh(II) and Ir(II) metals, 2,6-Pyridinedicarbonitrile, Tridentate N-donor ligand, Fluorescence, Antibacterial activity.

INTRODUCTION

Coordination compounds of transition metals show some important applications like medicinal properties, light emitting markers in biomedical fields and also to some extent of visible luminescence [1,2]. Due to adequate number of coordination sites and π -excessive nature of tetrazolates drift the visible luminescence predominantly [3]. Bipyridine, terpyridine bistetrazolate ligands and dicarboxylate analogous of lanthanide complexes have been reported to show visible luminescence properties [4,5]. The $f-f$ emission of some lanthanides covers the visible spectra for example Sm(III) pink, Dy(III) yellow, Eu(III) red and Tb(III) green. The tetrazoles as well as their derivatives containing high nitrogen percentage have been used in adsorption and luminescent materials [6]. The strong coordination ability of tetrazolate with d - and f -metal ions occurs due to excessive electron donor nitrogen atoms which also leads to display interesting photophysical properties [7]. The lanthanide complexes based on tetrazolates have strong ability to absorb UV-visible radiations which leads to coloured vision like OLEDs, waveguides and biomedical applications [8]. The bistetrazolate

polymers were increased extremely and covers wide applications including chemical sensors, luminescence and biomedicines [9]. Tetrazole photochemistry is itself rich, strongly affects their presence. The transition metal complexes of pyridine tetrazolate and pyridine tetrazolate oxide ($Hpytzo$, $Hpytz$) display extensive absorption spectra upto 412 nm with ruthenium [10]. The fluorescence spectra ($\lambda_{emission}$) of ligands ($Hpytzo$, $Hpytz$) was drifted upto 522 to 540 nm at 270 nm excitation wavelength as well as in metal complexes of Co (576 nm), Ni (554 nm) and Fe (522.5 nm). Thus, tetrazole derivatives significantly attracts attention towards various applications including luminescence [11]. Due to wide applications in material science and synthetic organic chemistry tetrazoles attract significant interest in recent times [12]. The emission spectra of lanthanides was efficiently sensitized by bistetrazolate pyridine ligands and also the absorption window was extended towards the visible region up to 330 nm [13]. In biological and material science applications, lanthanides stay great interest due to strong luminescent properties like selective probes [14]. With multidentate N and O-donor ligands, the photo-physical properties of Tb(III) complexes show strong absorption efficiency [15]. The nitrogen

containing derivatives were recognized useful structures to synthesize high energy materials including development of photo-luminescent materials [16,17]. The coordination polymers of tetrazolate pyridine oxide ligands with d^{10} metals attracts attention due to wide applications in the fields of fluorescence, catalysis [18]. The heavy metals and their complexes have been found profound role in antibacterial activity. Three binuclear Rh(II) complexes have been found more effective against *S. aureus* rather than *E. coli* [19]. The carbene-Rh(I) and Ru(II) complexes are found more active to inhibit the growth of *E. faecalis*, *S. aureus* at lower concentration than *E. coli* and *P. aeruginosa* [20]. The Ru(II) complexes showed mild to moderate antibacterial activity against some Gram-negative and Gram-positive bacterial strains whereas with *S. aureus*, methicillin resistant *S. aureus* (MRSA), *E. coli* and *K. pneumoniae* bacterial strains showed better activities [21,22].

EXPERIMENTAL

For experimental purpose all the materials were obtained from Sigma-Aldrich and Merck. The chemicals required for the study included rhodium trichloride trihydrate, iridium trichloride, 2,6-pyridinedicarbonitrile, triethylamine, sodium azide, methanol, ethanol, dimethyl sulphoxide, acetic acid, nutrient broth (peptone crystalline, sodium chloride, beef extract) and nutrient agar (peptone crystalline, sodium chloride, beef extract, *etc.*).

Characterization: The ligand and its metal complexes were characterized by analytical techniques. The elemental analysis of samples was performed by using Elemental Analyzer-EUROVECTOR EA 3000. The absorbance maxima (λ_{\max}) of samples was determined in DMSO using UV-VIS-NIR spectrometer-Shimadzu, UV-3600 plus. IR spectra of metal complexes from 4000 to 400 cm^{-1} was determined using FT-IR-Perkin-Elmer spectrum version 10.4.00. The chemical shift of metal complexes was recorded in δ ppm in DMSO- d_6 using NMR-JEOLCS-400. X-ray diffraction of complexes analysis was recorded in dried powder form using X-ray diffractometer-Rigaku, smart lab3kw. The fluorescence spectra of ligand and their complexes was recorded using Perkin-Elmer fluorescence spectrometer-LS 45 in DMSO and antibacterial activity of complexes was evaluated in DMSO.

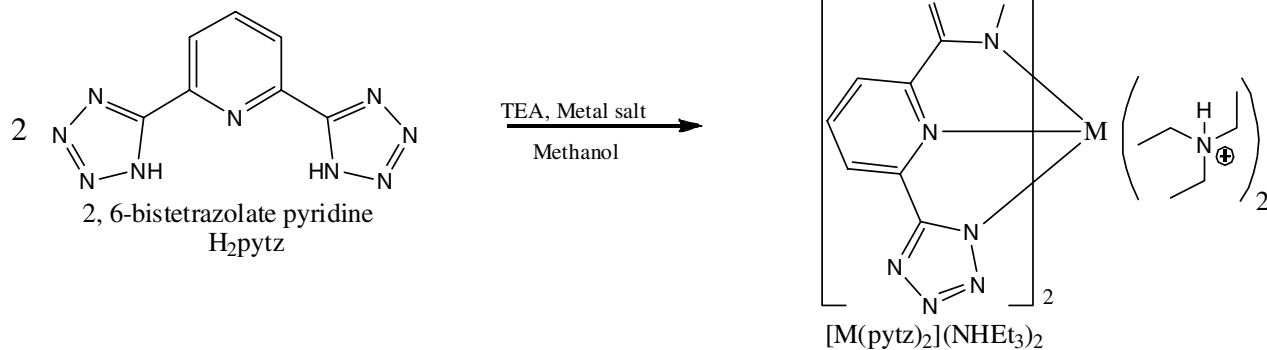
The spectra of metal complexes were plotted using Origin Lab OriginPro 9.0 Software. The molecular structure analysis

of metal complexes was performed by using ChemDraw Ultra 12.0 version software.

Synthesis of 2,6-bistetrazolate pyridine (H_2pytz): 2,6-Bistetrazolate pyridine was synthesized from 2,6-pyridinedicarbonitrile (1 g) by thermal cycloaddition reaction with sodium azide (2.53g) in presence of triethylamine (5.43 mL) and conc. HCl (1.2 mL) in toluene [10]. The compound was recovered by addition of water and acetic acid, after few minutes white powder of 2,6-bistetrazolate pyridine precipitate was obtained. Yield: 98 %, m.p.: 300 °C. Elemental analysis calcd. (found) (%) of $\text{C}_7\text{H}_5\text{N}_9\text{H}_2\text{O}$: C 38.86 (38.15), H 2.34 (2.25), N 56.59 (55.96). UV-visible: λ_{\max} 360 nm, abs. 2.366. Molar absorption coefficient (ϵ) = 473.2 $\text{M}^{-1} \text{cm}^{-1}$. FT-IR (KBr, cm^{-1}): 3570.5 (N-H str.), 3414.49 (O-H str.), 2925.23 (C-H str.), 1645.36 (C=C str.), 1604.13 (N=N str.), 1567.42 (C=N str.). ^1H NMR (400, MHz DMSO- d_6 , δ , ppm): 8.22-8.19 (s, 3H, pyr, $J = 12$ Hz), δ 5.70-5.68 (s, 1H, NH, $J = 8.0$ Hz), δ 3.21 peak of H_2O , δ 2.49-2.45 ($J = 4.0$ Hz) peak of CH_2 of NHET_3 , δ 2.01 (DMSO- d_6) and δ 1.14-1.10 ($J = 7.2$ Hz) peak of CH_3 of NHET_3 counter ion. Fluorescence ($\lambda_{\text{emission}}$): 539.5 nm at excitation wavelength 320 nm.

Synthesis of metal complexes: The metal complexes were synthesized from 2,6-bistetrazolate pyridine (H_2pytz) ligand in methanol as shown in **Scheme-I**. Briefly, 2,6-bistetrazolate pyridine (0.430 g) and 0.55 mL of triethylamine were dissolved in 20 mL methanol in 250 mL round bottom flask, then 0.264 g $\text{RhCl}_3 \cdot 3\text{H}_2\text{O}$ dissolved in 2 mL methanol was added. The reaction mixture was refluxed 12-16 h, dark brown coloured precipitate of metal complex ($\text{Rh}(\text{pytz})_2(\text{NHET}_3)_2$, **1**) appeared. The reaction mixture was cooled, filtered, washed with chilled water and then ethanol to remove salts. Yield: 50 %, m. p.: > 320 °C. Elemental analysis calcd. (found) (%) of $\text{C}_{26}\text{H}_{38}\text{N}_{20}\text{Rh} \cdot \text{H}_2\text{O}$: C 42.57 (42.17), H 5.22 (5.32), N 38.19 (39.15). FT-IR (KBr, cm^{-1}): 3428.67 (O-H str.), 2930.13 (C-H str.), 1634.57 (C=C str.), 1534.57 (N=N str.), 1408.20 (C=N str.), 1117.87 (N-H_b), 1032.25 (C-H_b), 823.54 (C-C str.) triethylamine, 428.67 (Rh-N str.). ^1H NMR (400 MHz, DMSO- d_6 , δ , ppm): 7.92 (3H, s, pyr), δ 3.54 peak of H_2O , δ 3.04-2.45 ($J = 6.8$ Hz) peak of CH_2 of NHET_3 , δ 2.45 (DMSO- d_6) and δ 1.10-1.07 ($J = 6.8$ Hz) peak of CH_3 group of NHET_3 counter ion.

Synthesis of $[\text{Ir}(\text{pytz})_2](\text{NHET}_3)_2$ (2**):** Complex **2** was synthesized in similar way as complex **1**, herein, 0.430 g of 2,6-bistetrazolate pyridine (H_2pytz) and 0.55 mL of triethyl-



Scheme-I: Synthesis of $[\text{M}(\text{pytz})_2](\text{NHET}_3)_2$ complexes (M = Rh, Ir)

RESULTS AND DISCUSSION

amine were dissolved in 20 mL methanol, then 0.299 g IrCl_3 dissolved in 2 mL methanol was added. Black coloured precipitate of metal complex (**2**) appeared. Yield: 55 %, m. p.: > 320 °C. Elemental analysis calcd. (found) (%) of $\text{C}_{26}\text{H}_{38}\text{N}_{20}\text{Ir}\cdot\text{H}_2\text{O}$: C 37.95 (38.12), H 4.65 (4.74), N 34.04 (34.89). FT-IR (KBr, cm^{-1}): 3370.07 (O-H str.), 2835.08 (C-H str.), 1638.03 (C=C str.), 1576.03 (N=N str.), 1408.08 (C=N str.), 1230.11 (N-H_b), 1169.23 (C-H_b), 826.11 (C-C str.) triethylamine, 440.41 (Ir-N str.). $^1\text{H NMR}$ (400 MHz, $\text{DMSO}-d_6$, δ , ppm): δ 8.83-8.80 (s, 3H, pyr $J = 9.6$ Hz), δ 3.35 peak of H_2O , δ 2.99-2.94 ($J = 7.2$ Hz) peak of CH_2 group of NHET_3 , δ 2.45 ($\text{DMSO}-d_6$) and δ 1.06-1.03 ($J = 7.2$ Hz) peak of CH_3 group of NHET_3 counter ion.

Antibacterial activity: An antibacterial activity of complexes was evaluated against four pathogenic bacterial species in DMSO using agar well diffusion method. Gram (-) bacteria: *Escherichia coli* & *Klebsiella pneumoniae* and Gram (+) bacteria: *Bacillus cereus* & *Staphylococcus aureus* bacterial species were obtained from Department of Industrial Microbiology and maintained in nutrient agar slant at 4 °C for further studies. Grown test bacterium were maintained on nutrient agar slant at 37 °C. The cultures was incubation for 3-days and utilized for test. The bacterial species were poured into four 250 mL conical flasks containing 150 mL of respective broth media and marked accordingly. The bacterial cultures were grown upto mid log growth phase. The grown bacterial cultures were incubated at 37 °C and appropriately maintained for further use.

The antibacterial activity of metal complexes was tested against Gram (-) and Gram (+) bacterial species by using agar well diffusion method. The nutrient agar media was prepared and autoclaved along with petriplates at 15 psi and 121 °C. After pouring the petriplates were allowed to solidify for 0.5 h. A 100 μL bacterial species was poured in petriplates separately and spread uniformly. Wells were prepared using sterile borer punched four well. The required concentration (2, 4 and 6 mg/mL) of samples was poured into well (size, 6 mm) by using micropipette and marked accordingly. The petriplates were incubated for 24 h to observe the bacterial growth and zone of inhibition (ZOI). After overnight incubation at 37 °C, different levels of ZOI were measured. The ZOI of samples were compared with the standard antibiotic-amoxicillin at 6 mg/mL concentration. The measurements were performed in triplicates to determine the mean of inhibition zone [23,24].

The solubility of ligand and its metal complexes increases in polar solvents methanol, ethanol and DMSO but were fairly soluble in chlorinated solvents. Both were thermally stable owing to low reactivity, resistant to pH changes and possess high melting point.

UV-visible studies: The absorption spectra of ligand and its metal complexes were recorded in DMSO (Fig. 1). The UV-visible spectra showed that tetrazole substituents influence greatly the absorption window of complexes towards longer wavelength in the visible region. The rhodium complex $[\text{Rh}(\text{pytz})_2](\text{NHET}_3)_2$ showed sharp absorption spectra (λ_{max}) at 367.2 nm (abs. 2.301, $\epsilon = 460.2 \text{ M}^{-1} \text{ cm}^{-1}$). While in the absorption spectra of iridium complex $[\text{Ir}(\text{pytz})_2](\text{NHET}_3)_2$, the tetrazolate rings showed pronounced effect λ_{max} 370.8 nm (abs. 2.678, $\epsilon = 535.2 \text{ M}^{-1} \text{ cm}^{-1}$). Hence, 2,6-bistetrazolate pyridine ligand (H_2pytz) extended the absorbance spectra towards the visible region with high absorption coefficient becomes useful tool in various applications like biomedical diagnostics as well as in optoelectronic devices.

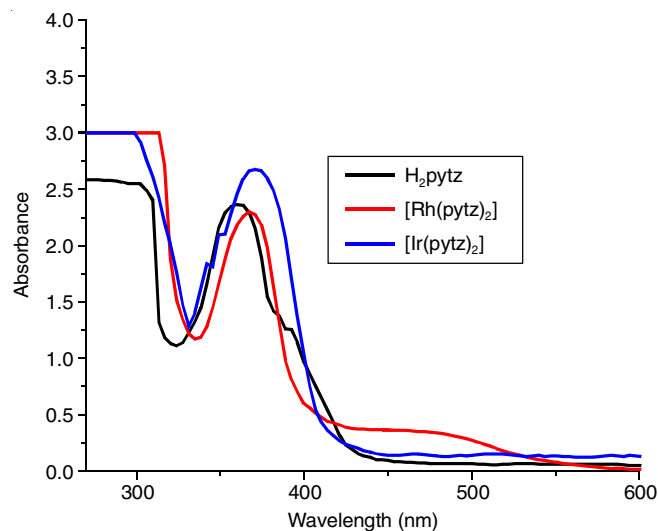


Fig. 1. UV-visible spectra of ligand (H_2pytz) and their complexes of Rh and Ir

FT-IR analysis: The FT-IR spectra of metal complexes $[\text{M}(\text{pytz})_2](\text{NHET}_3)_2$ ($\text{M} = \text{Rh}, \text{Ir}$) are shown in Fig. 2a-b. The absence of characteristic N-H stretching frequency of free

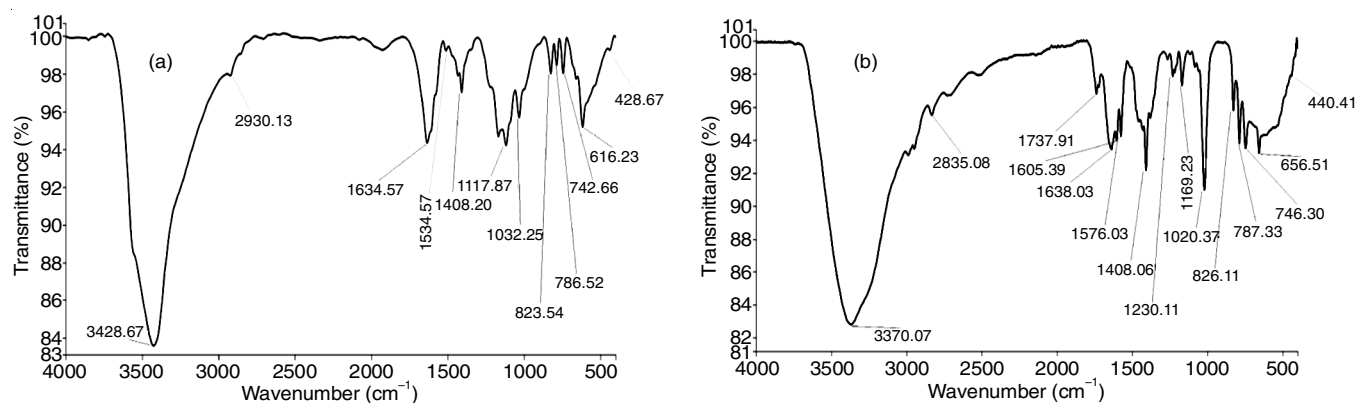


Fig. 2. FT-IR spectra of complexes (a) $[\text{Rh}(\text{pytz})_2](\text{NHET}_3)_2$ and (b) $[\text{Ir}(\text{pytz})_2](\text{NHET}_3)_2$

ligand determine the coordination with the metal centre. The presence of M-N stretching frequencies confirms the successful formation of metal complexes. The stretching frequency 3414.49 cm^{-1} in ligand (H_2pytz) confirms the O-H group of trapped water molecule as well as in complexes [10].

¹H NMR analysis: The ¹H NMR spectra of complexes of $[\text{M}(\text{pytz})_2](\text{NHEt}_3)_2$ ($\text{M} = \text{Rh}, \text{Ir}$) indicates the presence of characteristic C-H peaks of aromatic pyridine protons, whereas the absence of characteristic N-H peak of free ligand confirms the coordination with metal centre.

XRD analysis: The X-ray diffraction of spectra of metal complexes $[\text{M}(\text{pytz})_2](\text{NHEt}_3)_2$ ($\text{M} = \text{Rh}, \text{Ir}$) are shown in Fig. 3a-b. The diffraction studies was observed from angle (θ) between ($5\text{--}60^\circ$), wavelength ($\lambda = 0.154\text{ nm}$), radius (Rh, 0.134 nm , Ir, 0.136 nm) by using Cu $K\alpha$ radiations. The XRD spectra determines the presence of either one 4-fold or one 2-fold symmetry axis indicating two types of bravais lattices [primitive, body (end) centered]. The X-ray spectra revealed the characteristic monoclinic space group with six coordinated nitrogen atoms in $[\text{M}(\text{pytz})_2](\text{NHEt}_3)_2$ wraps the metal ion due to two deprotonated ligands [25]. The coordinated polyhedron is designated as trigonal cap like structure. The planarity of the complexes was explained on the basis of respective bond lengths and bond angles between the metal ion and coordinated ligands [17,26,27].

Molecular structure analysis: In the structure of metal complexes $[\text{M}(\text{pytz})_2](\text{NHEt}_3)_2$ ($\text{M} = \text{Rh}, \text{Ir}$), two deprotonated ligands coordinated with metal ion by four anionic nitrogen atoms of tetrazole units and two neutral nitrogen atoms of parent pyridine rings. The average bond distance involved by anionic tetrazole nitrogen atoms is 1.93165 \AA for (Rh-N),

1.95145 \AA for (Ir-N) and average bond distance involved due to neutral nitrogen atoms is 1.94 \AA for (Rh-N), 1.9596 \AA for (Ir-N). The bond angle between the metal ion and anionic tetrazolate nitrogen atoms is 144.7298° for N(13)-Rh-N(12) and 142.7210° for N(13)-Ir-N(12). The angle between neutral pyridine nitrogen atom, metal ion and tetrazolate nitrogen atom is 74.4409° for N(12)-Rh-N(3), 74.8300° for N(12)-Ir-N(3), whereas the angle between two neutral pyridine nitrogen atoms and metal ion is 172.6911° for N(19)-Rh-N(3), 171.3659° for N(19)-Ir-N(3). The selected bond distances and angles of metal complexes are given in Table-1 [27]. The metal ion lies in equatorial plane and situated on a two-fold symmetry axis defined by coordinating atoms N(3) of the ligand units. The metal ion were wrapped centrally by ligand units as shown in Fig. 4a-b, also furnishes protective surrounding from solvent interfaces [26,28].

Fluorescence studies: The fluorescence spectra of ligand (H_2pytz) (intense: 539.5 nm , abs. 703.4) and their metal complexes was recorded in solution at 298 K . The emission spectra of complexes $[\text{M}(\text{pytz})_2](\text{NHEt}_3)_2$ ($\text{M} = \text{Rh}, \text{Ir}$) was dominated through energy transfer process ($\text{L} \rightarrow \text{MCT}$) by highly energetic ligand (H_2pytz). A fluorescent spectra of complexes (Fig. 5) showed weak and intense peaks of varied intensities, the excitation wavelength at 330 nm , rhodium complex $[\text{Rh}(\text{pytz})_2](\text{NHEt}_3)_2$ display characteristic transition of 528.5 nm (abs. 921.3). Similarly, the excitation wavelength at 335 nm , iridium complex $[\text{Ir}(\text{pytz})_2](\text{NHEt}_3)_2$ exhibits specific transition of 557.5 nm (abs. 753.6) [11,15]. The π -electron releasing effect of bistetrazolate pyridine ligand strongly enhance the energy transition in the complexes through energy transfer process

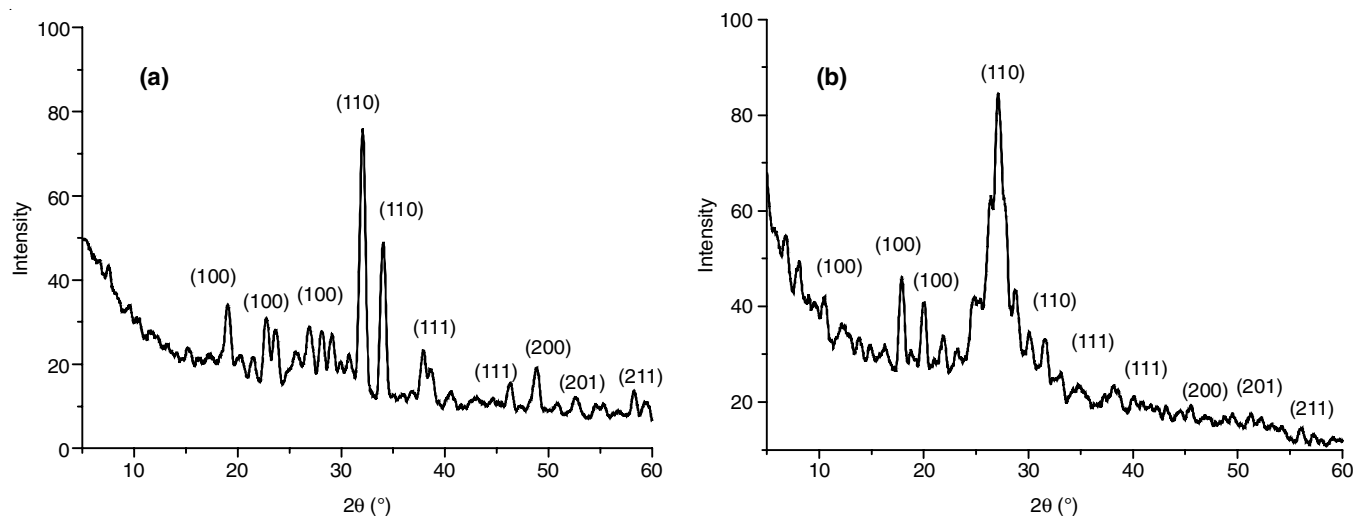


Fig. 3. XRD spectra of complexes of (a) $[\text{Rh}(\text{pytz})_2](\text{NHEt}_3)_2$ (b) $[\text{Ir}(\text{pytz})_2](\text{NHEt}_3)_2$

TABLE-1
SELECTED BOND DISTANCES AND ANGLES OF $[\text{Rh}(\text{pytz})_2](\text{NHEt}_3)_2$ AND $[\text{Ir}(\text{pytz})_2](\text{NHEt}_3)_2$ COMPLEXES

$[\text{Rh}(\text{pytz})_2]^{2-}$			$[\text{Ir}(\text{pytz})_2]^{2-}$				
Bond distance (\AA)		Bond angle ($^\circ$)	Bond distance (\AA)		Bond angle ($^\circ$)		
Rh(33)-N(19)	1.9405	N(19)-Rh-N(12)	107.2987	Ir(33)-N(19)	1.9601	N(19)-Ir-N(12)	109.6759
N(3)-Rh(33)	1.9395	N(19)-Rh-N(3)	172.6911	N(3)-Ir(33)	1.9591	N(19)-Ir-N(3)	171.3659
N(29)-Rh(33)	1.9291	N(13)-Rh-N(12)	144.7298	N(29)-Ir(33)	1.9487	N(13)-Ir-N(12)	142.7210
Rh(33)-N(28)	1.9334	N(13)-Rh-N(3)	75.4933	Ir(33)-N(28)	1.9532	N(13)-Ir-N(3)	74.8300
Rh(33)-N(13)	1.9313	N(12)-Rh-N(3)	74.4409	Ir(33)-N(13)	1.9512	N(12)-Ir-N(3)	73.7545
N(12)-Rh(33)	1.9328	N(29)-Rh-N(28)	150.6237	N(12)-Ir(33)	1.9527	N(29)-Ir-N(28)	149.2806

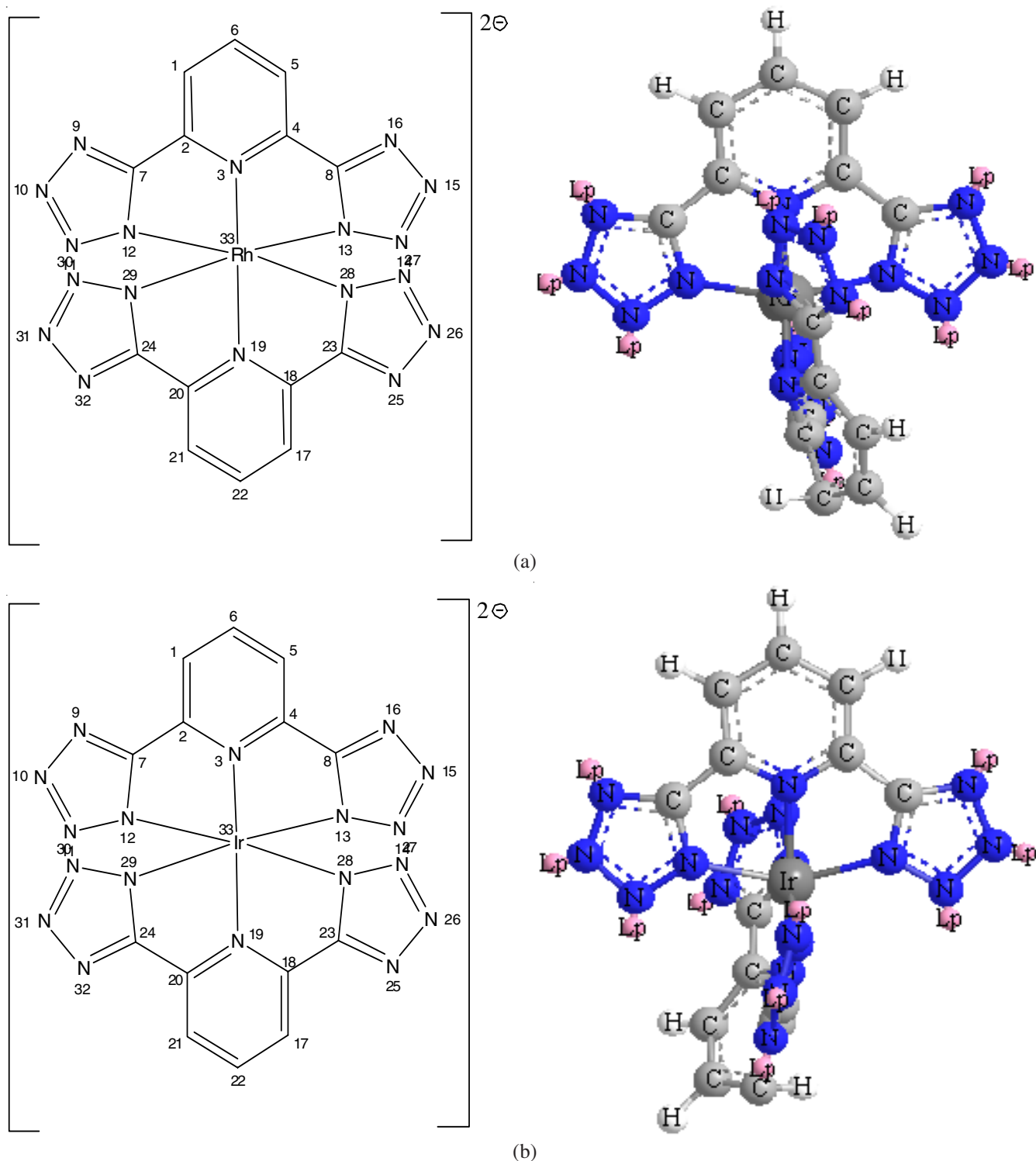


Fig. 4. Molecular structure of complexes of (a) $[\text{Rh}(\text{pytz})_2]^{2-}$ anion (b) $[\text{Ir}(\text{pytz})_2]^{2-}$ anion

which could lead to weak and intense visible emission spectra of complexes in the visible region [29].

Antibacterial activity: The current study evaluates the antibacterial activity of 2,6-bistetrazolate pyridine complexes of $[\text{M}(\text{pytz})_2](\text{NH}_4\text{Et}_3)_2$ ($\text{M} = \text{Rh}, \text{Ir}$) against four bacterial species using agar well diffusion method in DMSO. For negative control, the wells were loaded with DMSO whereas antibiotic- amoxicillin for positive control (6 mg/mL). The measurements of mean zone of inhibition was determined in triplicates

(excluded well diameter, 6 mm). The antibacterial data (Table-2) showed that $[\text{Rh}(\text{pytz})_2](\text{NH}_4\text{Et}_3)_2$ complex was found to be more active (*S. aureus*) than $[\text{Ir}(\text{pytz})_2](\text{NH}_4\text{Et}_3)_2$ complex (*E. coli*). It is observed that rhodium(II) complex was found more effective with maximum ZOI at 6 mg/mL concentration.

Conclusion

Rh(II) and Ir(II) complexes have been synthesized from tridentate nitrogen donor ligand (2,6-bistetrazolate pyridine).

TABLE-2
ANTIBACTERIAL ACTIVITY OF METAL COMPLEXES OF [Rh(pytz)₂](NHEt₃)₂,
[Ir(pytz)₂](NHEt₃)₂ AGAINST FOUR BACTERIAL SPECIES

Concentration (mg/mL)	Zone of inhibition diameter (mm)							
	[Rh(pytz) ₂](NHEt ₃) ₂				[Ir(pytz) ₂](NHEt ₃) ₂			
	<i>Escherichia coli</i>	<i>Klebsiella pneumoniae</i>	<i>Bacillus cereus</i>	<i>Staphylococcus aureus</i>	<i>Escherichia coli</i>	<i>Klebsiella pneumoniae</i>	<i>Bacillus cereus</i>	<i>Staphylococcus aureus</i>
Negative control	0	0	0	0	–	–	–	–
2	6.6 ± 1.52	7.3 ± 0.57	7.3 ± 0.57	9.3 ± 0.57	6.6 ± 0.57	6.3 ± 0.57	5.3 ± 0.57	5.6 ± 0.57
4	9.0 ± 1.00	9.3 ± 1.52	10.6 ± 2.08	12.0 ± 1.73	10.6 ± 1.15	11.0 ± 1.73	9.3 ± 1.15	9.3 ± 0.57
6	12.3 ± 0.57	13.3 ± 1.52	13.0 ± 1.73	15.3 ± 1.15	14.6 ± 1.15	13.3 ± 1.15	12.0 ± 1.73	12.6 ± 0.57
Positive control	–	–	–	–	27.3 ± 1.52	29.0 ± 1.73	26.6 ± 1.73	28.0 ± 1.52

Mean ± S.D, n = 3.

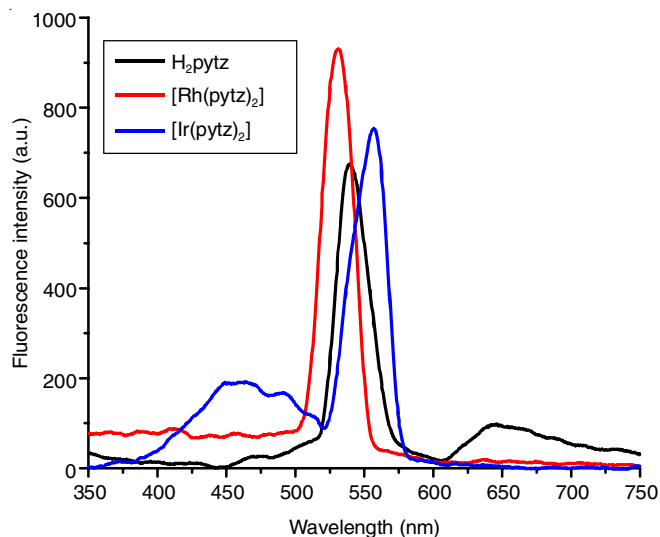


Fig. 5. Fluorescence spectra of ligand (H₂pytz) and their complexes of Rh and Ir

The structure of metal complexes was determined in solution (UV, ¹H NMR) as well as in solid state (FT-IR, XRD) and elemental analysis. The fluorescence spectra of complexes was efficiently sensitized with weak as well as sharp emission peaks in the visible region. The absorption spectra of complexes were also shifted towards the visible region upto 370.8 nm, both were desirable features in photo-physical applications. The antibacterial activity showed that rhodium and iridium complexes were found to be effective for Gram-positive as well as Gram-negative bacterial species, respectively. Therefore, tetrazolates present an excellent method for construction of new coordination design and also attracts attention in various applications ranging from photo-physical to biomedical fields.

ACKNOWLEDGEMENTS

The research work is authentic and original supported by Young Scientists of Department of Chemistry, Faculty of Science, Sam Higginbottom University of Agriculture, Technology and Sciences and Motilal Nehru National Institute of Technology, Allahabad, India.

CONFLICT OF INTEREST

The authors declare that there is no conflict of interests regarding the publication of this article.

REFERENCES

- J.C.G. Bunzli and C. Piguet, *Chem. Soc. Rev.*, **34**, 1048 (2005); <https://doi.org/10.1039/b406082m>.
- S. Comby and G.J.-C. Bunzli, *Handbook on the Physics and Chemistry of Rare Earths*, Elsevier: Amsterdam, p. 37 (2007).
- G.X. Wang and Y.W. Zhang, *Inorg. Chim. Acta*, **376**, 212 (2011); <https://doi.org/10.1016/j.ica.2011.06.016>.
- M. Giraud, E.S. Andreiadis, A.S. Fisyuk, R. Demadrille, J. Pecaut, D. Imbert and M. Mazzanti, *Inorg. Chem.*, **47**, 3952 (2008); <https://doi.org/10.1021/ic8005663>.
- A.-L. Gassner, C. Duhot, J.-C. G. Bünzli and A.-S. Chauvin, *Inorg. Chem.*, **47**, 7802 (2008); <https://doi.org/10.1021/ic800842f>.
- G.W. Yang, Y.T. Zhang, Q. Wu, M.J. Cao, J. Wu, Q.Y. Yue and Q.Y. Li, *Inorg. Chim. Acta*, **450**, 364 (2016); <https://doi.org/10.1016/j.ica.2016.06.015>.
- H. Zhao, Z.-R. Qu, H.-Y. Ye and R.-G. Xiong, *Chem. Soc. Rev.*, **37**, 84 (2008); <https://doi.org/10.1039/B616738C>.
- K. Kuriki, Y. Koike and Y. Okamoto, *Chem. Rev.*, **102**, 2347 (2002); <https://doi.org/10.1021/cr010309g>.
- U. Sheridan, J.F. Gallagher and J. McGinley, *Inorg. Chim. Acta*, **450**, 263 (2016); <https://doi.org/10.1016/j.ica.2016.06.011>.
- R.A. Malik, N.G. Bhat, R. Yadav, N. Singh, G. Kumar and S. Mal, *Asian J. Chem.*, **30**, 2159 (2018); <https://doi.org/10.14233/ajchem.2018.21056>.
- T. Hu, L. Liu, X. Lv, X. Chen, H. He, F. Dai, G. Zhang and D. Sun, *Polyhedron*, **29**, 296 (2010); <https://doi.org/10.1016/j.poly.2009.05.015>.
- F. Dehghani, A.R. Sardarian and M. Esmailpour, *J. Organomet. Chem.*, **743**, 87 (2013); <https://doi.org/10.1016/j.jorganchem.2013.06.019>.
- E.S. Andreiadis, D. Imbert, J. Pécaut, R. Demadrille and M. Mazzanti, *Dalton Trans.*, **41**, 1268 (2012); <https://doi.org/10.1039/C1DT11627D>.
- P. Gawryszewska, J. Sokolnicki, A. Dossing, J.P. Riehl, G. Muller and J. Legendziewicz, *J. Phys. Chem.*, **109**, 3858 (2005); <https://doi.org/10.1021/jp0444666>.
- X.Q. Song, G.Q. Cheng and Y.A. Liu, *Inorg. Chim. Acta*, **450**, 386 (2016); <https://doi.org/10.1016/j.ica.2016.06.028>.
- P.C.R. Soares-Santos, H.I.S. Nogueira, V. Félix, M.G.B. Drew, R.A. Sá Ferreira, L.D. Carlos and T. Trindade, *Chem. Mater.*, **15**, 100 (2003); <https://doi.org/10.1021/cm021188j>.
- G. Pompidor, A. Daleo, J. Vicat, L. Toupet, N. Giraud, R. Kahn and O. Maury, *Angew. Chem. Int. Ed.*, **47**, 3388 (2008); <https://doi.org/10.1002/anie.200704683>.
- M. Cheng, Y.S. Ding, Z. Zhang and Q.X. Jia, *Inorg. Chim. Acta*, **450**, 1 (2016); <https://doi.org/10.1016/j.ica.2016.05.016>.
- P.P. Florian, B. Magorzata and L. Tadeusz, *Met. Based Drugs*, **3**, 186 (1996).
- C. Bekir, C. Engin, K. Hasan and D. Riza, *J. Med. Sci. (Dacca)*, **46**, 821 (1997).

21. U.K. Mazumder, M. Gupta, S. Bhattacharya, S.S. Karki, S. Rathinasamy and S. Thangavel, *J. Enzyme Inhib. Med. Chem.*, **19**, 185 (2004); <https://doi.org/10.1080/14756360310001650192>.
22. A. Abebe and H. Hailemariam, *Bioinorg. Chem. Appl.*, **2016**, Article ID 3607924 (2016); <https://doi.org/10.1155/2016/3607924>.
23. M.M. Tania, F.A. Silva, M. Brando, M.T. Grandi and A.F.F. Smania, *J. Herbs Spices Med. Plants*, **11**, 1 (2000).
24. N. Ahmad, F. Anwar, S. Hameed and C.M. Boyce, *J. Med. Plants Res.*, **5**, 4879 (2011).
25. E.S. Andreiadis, R. Demadrille, D. Imbert, J. Pécourt and M. Mazzanti, *Chem. Eur. J.*, **15**, 9458 (2009); <https://doi.org/10.1002/chem.200900912>.
26. J. Albertsson, D.G. Nicholson, A.D. Mukherjee, K. Nilsson and W. Nimmich, *Acta Chem. Scand.*, **26**, 985 (1972); <https://doi.org/10.3891/acta.chem.scand.26-0985>.
27. C. Gateau, M. Mazzanti, J. Pecaut, F.A. Dunand and L. Helm, *Dalton Trans.*, 2428 (2003); <https://doi.org/10.1039/B303079B>.
28. P.A. Brayshaw, J.-C.G. Buenzli, P. Froidevaux, J.M. Harrowfield, Y. Kim and A.N. Sobolev, *Inorg. Chem.*, **34**, 2068 (1995); <https://doi.org/10.1021/ic00112a019>.
29. G.S. Kottas, M. Mehlstäubl, R. Fröhlich and L. De Cola, *Eur. J. Inorg. Chem.*, 3465 (2007); <https://doi.org/10.1002/ejic.200700514>.